Dalton Transactions

ROYAL SOCIETY OF CHEMISTRY

PAPER

View Article Online
View Journal | View Issue

Cite this: *Dalton Trans.*, 2020, **49**, 6127

Synthesis and reactivity of nitridorhenium complexes incorporating the mercaptoethylsulfide (SSS) ligand†

Nikola S. Lambic, Roger D. Sommer and Elon A. Ison *

Received 19th February 2020,
Accepted 16th April 2020

DOI: 10.1039/d0dt00631a

rsc.li/dalton

A method for the preparation of nitridorhenium(v) complexes of the form (SSS)Re(N)(L) (where SSS = 2-mercaptoethylsulfide and L = PPh_3 and *t*-BuNC) has been described. These complexes react with Lewis acids allowing for the isolation of adducts. The lack of a significant steric profile on the SSS ligand combined with enhanced nucleophilicity of the nitrido group does not allow for the effective formation of frustrated Lewis pairs with these complexes and as a result these species are poor catalysts for the hydrogenation of unactivated olefins.

Introduction

Oxorhenium complexes have been studied extensively because of their ability to catalyze a variety of chemical transformations including a variety of organic oxidations,[1] hydrosilylations,[2] deoxygenations,[3] didehydroxylations,[4] and C–O[5] and C–C[6] bond forming reactions. In contrast, the chemistry of nitridorhenium complexes is not developed as well for catalytic applications.

Recently, our group has demonstrated that oxorhenium complexes can be utilized as the Lewis base component of frustrated Lewis pairs and that these species can be utilized as catalysts for the hydrogenation of unactivated olefins.[7] Compared to the oxo group, nitrido ligands are expected to be more nucleophilic, and may allow for the development of FLP catalysts with Lewis acids that are functional group tolerant.[8]

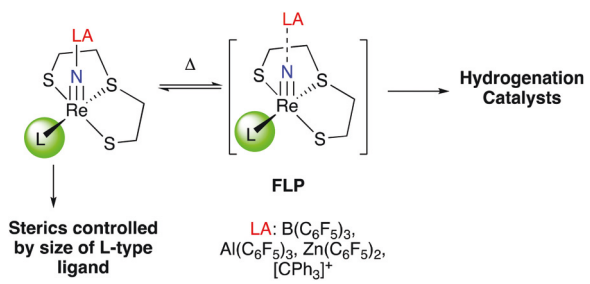

Fig. 1 Strategy for the generation of frustrated Lewis pairs from nitridorhenium complexes featuring mercaptoethylsulfide (SSS) ligands.

Department of Chemistry, North Carolina State University, 2620 Yarbrough Drive, Raleigh, North Carolina 27695-8204, USA. E-mail: eaison@ncsu.edu

†Electronic supplementary information (ESI) available: Crystallographic data. CCDC 1983930–1983932. For ESI and crystallographic data in CIF or other electronic format see DOI: 10.1039/d0dt00631a

As a result we were interested in the development of nitridorhenium species that may act as catalysts. Nitridorhenium species have been synthesized with a variety of ligands and have been utilized in many stoichiometric reactions.[8,9] Generally, the nitrido groups in these species exhibit nucleophilic character and can be isolated with a variety of electrophiles.[10] For our initial FLP catalysts we utilized five-coordinate pseudo-square pyramidal rhenium complexes with an oxo group occupying the apical position. The ambiphilic nature of the oxo group[11] as well as its strong tendency to discourage trans ligation[12] enabled us to develop hydrogenation catalysts that activate the substrate at the oxo ligand rather than at the metal center. Sterics were controlled in these complexes by manipulating the size of the X-type ligand attached to rhenium.[7]

In order to synthesize similar complexes with nitrido ligands a similar approach was employed. The SSS (SSS = 2-mercaptoethylsulfide) ligand was utilized. However, the general structure of these complexes differ from the oxorhenium analogues in that an L-type ligand is present in the primary coordination sphere of rhenium. In a strategy similar to frustrated Lewis pairs with oxorhenium complexes, the sterics on this L-type ligand may be used to induce FLP reactivity (Fig. 1).

Results and discussion

Complex (SSS)Re(N)PPh_3, **1**, was synthesized by ligand substitution of one PPh_3 and two Cl-ligands of $(PPh_3)_2Re(N)Cl_2$ with the SSS (SSS = 2-mercaptoethylsulfide) ligand (Scheme 1). Complex **1** was characterized by several spectroscopic methods, including ^1H, ^{13}C and ^{31}P NMR, FTIR spectroscopy, and X-ray crystallography. The diastereotopic nature of the methylene backbone of the SSS ligand is evident in the ^1H

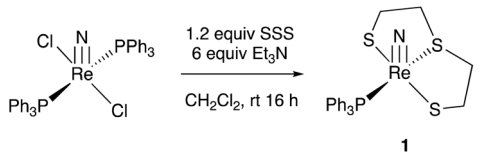

Scheme 1 Synthesis of (SSS)Re(N)PPh_3, **1**.

NMR spectrum of **1** as three signals (two overlapping) corresponding to the magnetically inequivalent protons were observed as complex multiplets due to the second order coupling. The PPh_3 ligand was detected in the ^{31}P NMR spectrum as a singlet resonating at 33.0 ppm. These spectral data are consistent with the nitrido complexes previously synthesized by Duatti and coworkers.[13]

Reactivity of 1 with electrophiles

Lewis acid/base adducts. The reactivity of nitridorhenium species with electrophiles has some precedent, as a variety of donor–acceptor complexes have been isolated.[10] Complex **1** reacts in a similar fashion with perfluorinated Lewis acids, such as $B(C_6F_5)_3$, $Al(C_6F_5)_3$, and $Zn(C_6F_5)_2$ to afford Lewis acid/base adducts **2a**, **2b**, **2c** respectively (Scheme 2).

Compared to the analogous adducts with oxorhenium complexes, this red compound, **2a**, shows remarkable stability to moisture and air, and is thermally stable up to 120 °C. For example, the corresponding $B(C_6F_5)_3$ adduct of (SSS)Re(O)Me was found to undergo rapid decomposition at elevated temperatures (80–100 °C) under an O_2 atmosphere. The disparate reactivity suggests that the Re–N–B interaction may be stronger than the Re–O–B interaction in the oxo analogs.

By ^{19}F NMR spectroscopy, three signals were observed for the symmetrically equivalent fluorine nuclei of the Lewis acid. The characteristic signals at −131.04, −160.36 and −165.75 ppm are shifted up field compared to the parent $B(C_6F_5)_3$ and indicate the formation of an adduct through the boron center. The PPh_3 signal was observed at 30.9 ppm in **2a** by ^{31}P NMR spectroscopy, which is shifted upfield from **1** where the analogous signal was observed at 33.0 ppm.

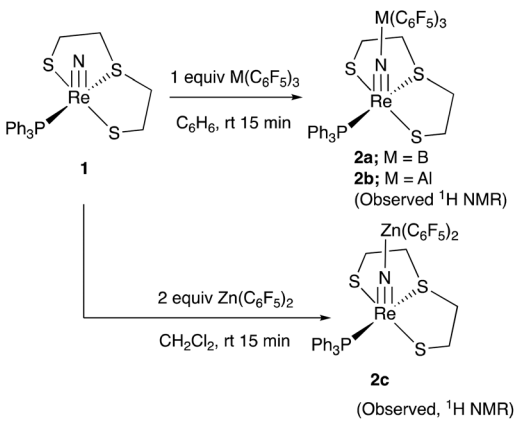

Scheme 2 Reactions of **1** with electrophiles.

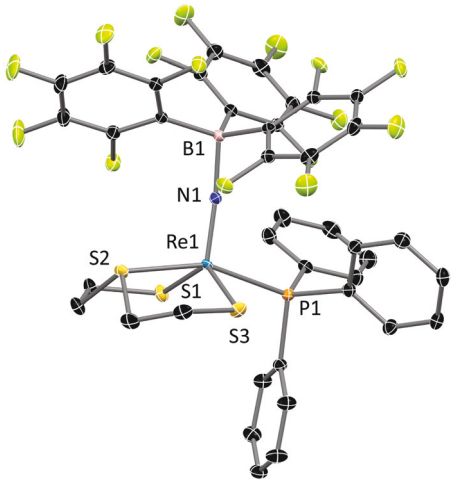

Fig. 2 Thermal ellipsoid plot for **2a** (50% ellipsoids). Selected bond lengths (Å) and angles (°). Re1–N1, 1.697(2); Re1–S1, 2.3819(6); Re1–S3, 2.3074(5); Re1–S2, 2.3099(5); Re1–P1, 2.4430(6); N1–B1, 1.586(3); Re1–N1–B1, 173.2(1).

X-ray crystal structure of 2a. Vapor diffusion of pentane into a concentrated methylene chloride solution of **2a** resulted in X-ray quality crystals (Fig. 2). On the basis of τ value (0.44) the geometry around the rhenium center is best described as intermediate between trigonal bipyramidal and square pyramidal with the N–$B(C_6F_5)_3$ moiety in the apical position. The Re–N bond length is not substantially elongated (1.697(2) Å) indicating that triple bond character is maintained in complex **2a**.

Nucleophilic reactivity of rhenium nitrido species has been reported. For example, Green and coworkers were able to isolate and structurally characterize a $B(C_6F_5)_3$ adduct of [Re(N)$(PR_3)(S_2CNR'_2)_2$] with the Re–N and B–N bond lengths in good agreement with **2a**.[14] In **2a**, $B(C_6F_5)_3$ is not easily displaced by other nucleophiles (such as phosphines and isocyanides), indicative of the strength of the new nitrido–boron bond.

Synthesis of cationic rhenium imido complexes. Complex **1** was found to be unreactive towards common organic electrophiles such as methyl iodide (MeI) or benzyl chloride (BnCl). However treatment of **1** with trityl tetrafluoroborate in benzene afforded the tritylimido rhenium complex **3** (Scheme 3).

Similar to previous complexes bearing the SSS ligand, the chemical shifts of the diastereotopic protons on the ethylene backbone are diagnostic.[12c] For example, complex **3** has four clearly resolved complex multiplets, each belonging to the symmetrically inequivalent methylene protons of the SSS ligand. The phosphine signal is observed at 31.0 ppm by ^{31}P NMR spectroscopy while the presence of the tetrafluoroborate counterion was observed at −155.0 ppm in the ^{19}F NMR spectrum. The ability of nitridorhenium complexes to bind carbon electrophiles has been noted by Kirmse[10a,b] and Leung,[15] and both groups were able to characterize rhenium tritylimido complexes.

X-ray crystal structure of 3. Vapor diffusion of pentane into a CH_2Cl_2 concentrated solution of **3** afforded crystals suitable

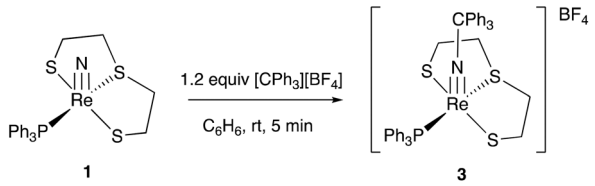

Scheme 3 Synthesis of [(SSS)Re(NCPh$_3$)(PPh$_3$)][BF$_4$], **3**.

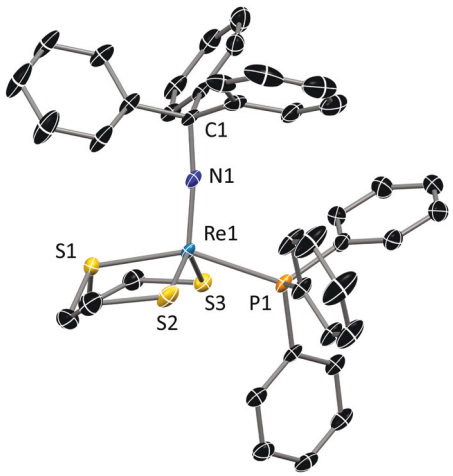

Fig. 3 Thermal ellipsoid plot for the cation in[(SSS)Re(NCPh$_3$)(PPh$_3$)][BF$_4$], **3**. (50% ellipsoids). Selected bond lengths (Å) and angles (°). Re1–N1, 1.709(4); Re1–S1, 2.3712(9); Re1–S3, 2.302(1); Re1–S2, 2.299(1); Re1–P1, 2.433(1); N1–C1, 1.473(6); Re1–N1–C1, 173.0.

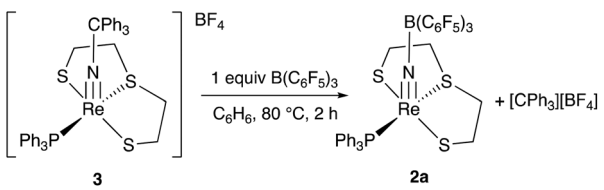

Scheme 4 Reaction of **3** with B(C$_6$F$_5$)$_3$.

for X-ray analysis. The X-ray crystal structure of **3** is shown in Fig. 3. The geometry around rhenium center is best described as distorted square pyramidal (τ = 0.33) with the imido ligand in the apical position. The Re–nitrogen bond is slightly longer (1.71 Å) than that of the parent nitrido complex (1.68 Å), and can still be considered a triple bond. Other bond lengths are in good agreement with previous structures bearing the same ligand set.[12c]

When B(C$_6$F$_5$)$_3$ was added to the solution of **3**, substitution at the nitrogen atom was observed and the product of the reaction was **2a** (Scheme 4).

Reactivity of 1 with nucleophiles

With the nucleophilic behavior of the nitrido moiety established, we turned our attention towards investigating the nucleophilic substitution of phosphine by a variety of ligands

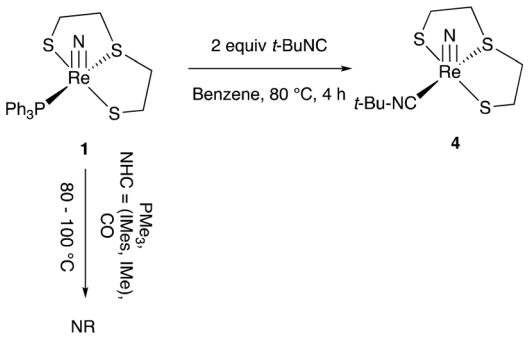

Scheme 5 Ligand substitution reactions with **1**.

as it allows for tuning of nucleophilicity by installing different ligands that can affect the donor/acceptor properties of the Re≡N bond and it also allows for tuning of sterics around the Re≡N bond which can result in the generation of frustrated Lewis pairs as in the analogous oxorhenium systems.

When σ-donating ligands such as PMe$_3$ or N-heterocyclic carbene (NHC = (IMes) = 1,3-dimesityl-2,3-dihydro-1*H*-imidazol-2-ylidene, or (IMe) = 1,3-dimethyl-2,3-dihydro-1*H*-imidazol-2-ylidene) were allowed to react with **1** at elevated temperatures, no reaction was observed. Similarly carbon monoxide did not react with **1** (Scheme 5).

However, when two equivalents of *t*-BuNC was heated at reflux with **1** in benzene, ligand substitution was observed and the resulting red complex, **4**, was isolated and characterized (Scheme 5). The PPh$_3$ ligand was not observed by ^{1}H and ^{31}P NMR spectroscopy, while the *t*-Bu group on the isonitrile ligand was observed as a singlet at 0.7 ppm by ^{1}H NMR spectroscopy. A very sharp isocyanide stretch at 2172 cm^{-1} was observed by FTIR spectroscopy.

The isocyanide ligand is a weaker π acceptor than CO, and the isocyanide stretch in the case of **4** is actually shifted to higher wavenumbers (relative to free *t*-BuNC (2132 cm^{-1})), indicating that σ donation from *t*-BuNC to Re is the dominant interaction in the complex. The Re≡N stretching frequency in **4** is lower (1055 cm^{-1}) compared to the starting material **1** (1094 cm^{-1}) as a result of the increased electron density on the metal in the isocyanide complex.

Kinetics of substitution

Since complex **1** is a square pyramidal, 16 electron complex, phosphine substitution by isocyanide is expected to proceed *via* an associative interchange mechanism. Furthermore, the presence of the terminal nitrido ligand trans to the open coordination site could potentially affect the overall mechanism of substitution. In order to confirm the type of substitution, kinetic studies were performed. The kinetic data are presented in Fig. 4.

From the kinetic plot in Fig. 4, product formation is exponential, indicating a first order dependence on rhenium. Under pseudo first order conditions the rate law is described by eqn (1). A plot of k_{obs} against varying [*t*-BuNC] is linear with a zero intercept (eqn (2)), indicating a first order dependence

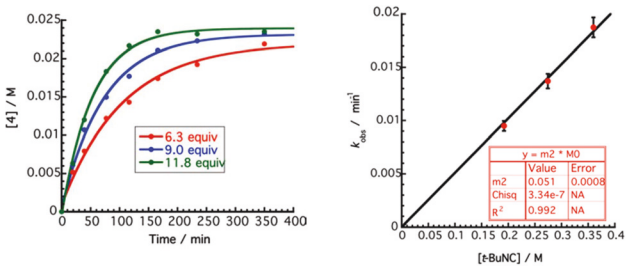

Fig. 4 Kinetics of PPh_3 substitution. Time profiles for the formation of **4** from **1** and *t*-BuNC over varying concentrations of *t*-BuNC (left plot). Plot of k_{obs} *vs.* [*t*-BuNC] (right plot). Conditions: [**1**] = 0.0305 M, [*t*-BuNC] = 0.192 M (6.3 equiv.), 0.275 M (9.0 equiv.), 0.360 M (11.8 equiv.). Concentrations were determined by ^{1}H NMR spectroscopy with mesitylene as the internal standard. Reactions were performed at 55 °C in benzene, k_{obs} = 9.4(0) × 10^{-3} min^{-1} (6.3 equiv.); 1.3(1) × 10^{-2} min^{-1} (9.0 equiv.); k_{obs} = 1.9(1) × 10^{-2} min^{-1} (11.8 equiv.). Data (left panel) are fit to the exponential function: [**4**] = *m*1 + *m*2 × (1 − exp(−*m*3 × *x*)).

on the incoming ligand as well. Therefore, the rate law exhibits first order dependencies on both **1** and [*t*-BuNC]. The rate law for the reactions is described by eqn (3).

$$\frac{-\mathrm{d}[\mathbf{1}]}{\mathrm{d}t} = \frac{\mathrm{d}[\mathbf{4}]}{\mathrm{d}t} = k_{obs}[\mathbf{1}] \quad (1)$$

$$k_{obs} = k_2[t\text{-BuNC}] \quad (2)$$

$$\frac{-\mathrm{d}[\mathbf{1}]}{\mathrm{d}t} = \frac{\mathrm{d}[\mathbf{4}]}{\mathrm{d}t} = k_2[\mathbf{1}][t\text{-BuNC}] \quad (3)$$

In order to gain a better understanding of transition state energetics, temperature dependence experiments were conducted. Time profiles for three separate runs and the resulting Eyring plot are depicted in Fig. 5.

Temperature dependence data described are consistent with associative interchange substitution mechanism (Scheme 6) for the reaction of **1** with *t*-BuNC. The entropy of activation is large and negative and is indicative of the ordered nature of the transition state.

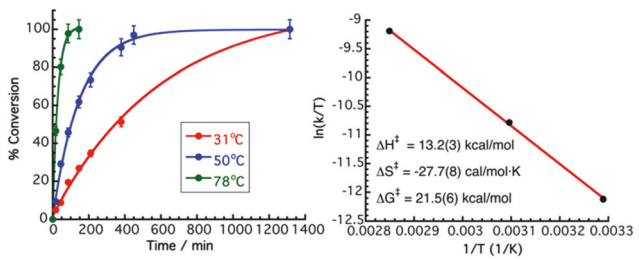

Fig. 5 Temperature dependence data. Time profiles for formation of **4** over time with varying temperature (left) and the Eyring plot (right). Conditions: [**1**] = 0.0305 M, [*t*-BuNC] 0.305 M (10 equiv.). Conversions determined by ^{1}H NMR spectroscopy by integrating the ratio of PPh_3 ligand peaks in complex **1** against free PPh_3. k_{obs} = 1.6(1) × 10^{-3} min^{-1} (31 °C); k_{obs} = 6.7(3) × 10^{-3} min^{-1} (50 °C); k_{obs} = 3.6(1) × 10^{-2} min^{-1} (78 °C).

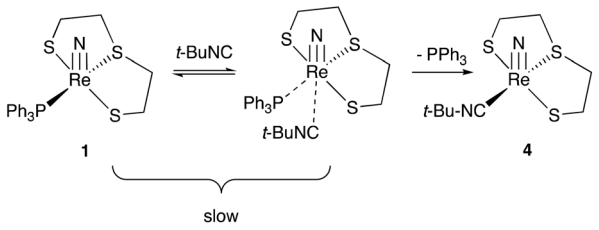

Scheme 6 Proposed mechanism for substitution reactions with **1**.

Computational studies

In order to understand the bonding of the *t*-BuNC ligand, DFT (M06)[16] calculations were performed on **1** and **4**. These two complexes are the same geometry but differ in the nature of the L-type ligand bound to rhenium (PPh_3 in **1** and *t*-BuNC in **4**). As shown in Fig. 6, the HOMO and LUMO for both complexes are similar. However, the HOMO for **4** includes significant electron density on the *t*-BuNC group reflecting significant π-back bonding. In addition, the LUMO is destabilized by mixing of the isocyanide π* orbital with the antibonding component of the Re≡N π bond.

Calculations suggest the isocyanide ligand in **4** is stabilized by π-backbonding to rhenium. However the net stabilization due to the isocyanide ligand acting as a π acceptor is small. This is reflected in the small difference in the HOMO–LUMO gap between **1** and **4** (0.09 eV). These data are also consistent with the IR data for **4** (*vide supra*) where it was observed that νCN band was observed at higher wavenumbers than free *t*-BuNC. This suggests that the major stabilization of the isocyanide ligand is σ donation and not π-backbonding.

X-ray crystal structure of 4. The thermal ellipsoid plot for **4** is depicted in Fig. 7. The Re–C bond in **4** (2.055 Å) is typical for similar Re complexes.[1a,17] Other bond distances are also

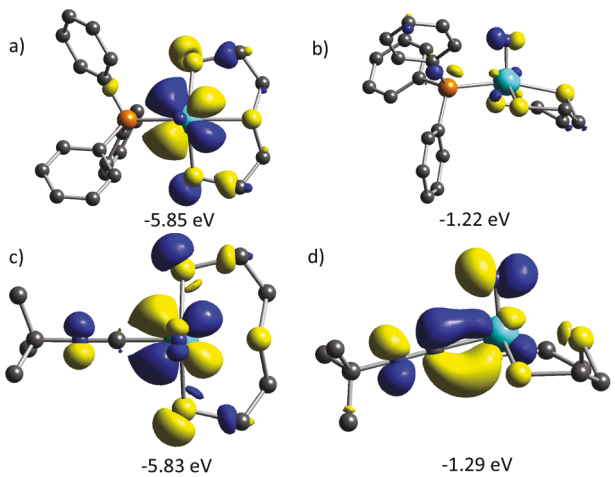

Fig. 6 Kohn–Sham Orbitals (M06) for complexes **1** and **4**. (a) HOMO of **1**, (b) LUMO of **1** (c) HOMO of **4**, (d) LUMO of **4**.

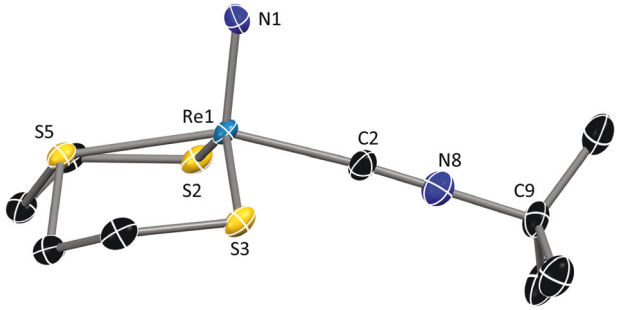

Fig. 7 Thermal ellipsoid plot (50% ellipsoids) for **4**. Selected bond lengths (Å) and angles (°): Re1–N1, 1.664(4); Re1–C1, 2.055(5); Re1–S2, 2.359(1); Re1–S3, 2.355(1); Re1–S1, 2.390(1); C1–N2, 1.144(7); Re1–C1–N2, 175.8(4).

within the normal range for similar nitridorhenium complexes and the metal center is best described as in a distorted square pyramidal environment ($\tau = 0.35$).[13]

Reactions of 4 with Lewis acids

Similar to **1**, complex **4** reacts cleanly with the Lewis acids $M(C_6F_5)_3$ (M = B and Al) to yield adducts (Scheme 7). These reactions again exemplify the nucleophilic nature of the nitrido group in these complexes.

Hydrogenation catalysis

To examine the potential catalytic activity of these complexes we examined the hydrogenation of 3,3-dimethylbut-1-ene with **1** as a catalyst in the presence of the Lewis acids $B(C_6F_5)_3$, $Al(C_6F_5)_3$ and $HB(C_6F_5)_2$ (Table 1). We have previously shown that oxorhenium complexes can act as the Lewis base component of frustrated Lewis pairs and are effective as catalyst for the hydrogenation of unactivated olefins.[7]

As shown in Table 1 catalysis with the nitridorhenium complexes reported here was poor for the hydrogenation of 3,3-dimethylbut-1-ene. These results are consistent with the hypothesis that repulsive steric interactions on the ancillary ligand in these complexes are important for the development of frustrated Lewis pairs. The absence of sterically demanding groups on the 2-mercaptoethylsulfide ligand, in addition to the stronger nucleophilicity of nitrido groups compared to oxo ligands in oxorhenium based FLPs, make these complexes less effective catalysts for this reaction.

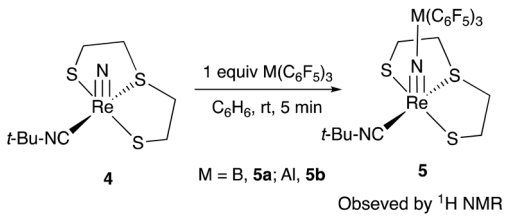

Scheme 7 Synthesis of adducts **5**.

Table 1 Hydrogenation of 3,3-dimethylbut-1-ene with **1** in the presence of Lewis acids[a]

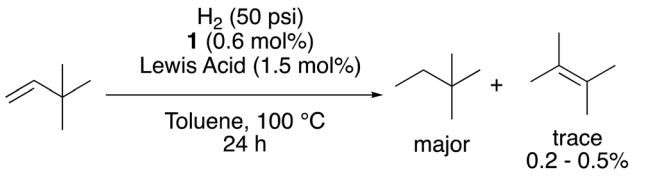

Lewis acid	% conversion	TON	TOF
$B(C_6F_5)_3$	Trace	—	—
$Al(C_6F_5)_3$	Trace	—	—
$HB(C_6F_5)_2$	10	17	0.71 h^{-1}

[a] Conditions: **1** = 0.0046 mmol; Lewis acids, 0.0112 mmol; 3,3-dimethylbut-1-ene, 0.776 mmol. Reactions were analyzed by ^1H NMR spectroscopy.

Conclusions

A method for the preparation of nitridorhenium(v) complexes of the form (SSS)Re(N)(L) (where SSS = 2-mercaptoethylsulfide and L = PPh_3 and *t*-BuNC) has been described. Consistent with previously reported reactivity, the nitrido ligand is nucleophilic, allowing for the isolation of adducts with Lewis acids. The lack of a significant steric profile on the SSS ligand combined with enhanced nucleophilicity of the nitrido group does not allow for the effective formation of frustrated Lewis pairs with these complexes and as a result these species are poor catalysts for the hydrogenation of unactivated olefins.

Experimental section

General considerations

Complex $Re(N)(PPh_3)_2(Cl)_2$ [18] was prepared as previously reported; all other reagents were purchased from commercial resources and used as received. $B(C_6F_5)_3$ was purchased from Strem Chemicals and sublimed prior to use. ^1H, ^{13}C, ^{19}F NMR spectra were obtained on 300 or 400 MHz spectrometers at room temperature. Chemical shifts are listed in parts per million (ppm) and referenced to their residual protons or carbons of the deuterated solvents respectively. All reactions were run under an inert atmosphere with dry solvents unless otherwise noted. FTIR spectra were obtained in KBr thin films. Elemental analyses were performed by Atlantic Micro Labs, Inc.

Synthesis of 1. In a 25 ml scintillation vial, $(PPh_3)_2Re(N)Cl_2$ (500 mg, 0.63 mmol) and Et_3N (6 equiv. 3.78 mmol) were dissolved in 10 ml CH_2Cl_2. The SSS ligand (2,2 thiodiethanethiol) (1.5 equiv. 0.95 mmol, 0.12 ml) was added to the reaction mixture, which was allowed to stir at room temperature for 1 h. Solvent was removed under reduced pressure and the following yellow residue was redissolved in minimal amount of CH_2Cl_2. Addition of excess hexanes resulted in precipitation of a yellow powder, which was washed with methanol on a filter

frit and dried *in vacuo*. Isolated (240 mg, 62% yield). ^{1}H NMR (CD_2Cl_2) δ: 7.74 (m, 5H, PPh_3–Phenyl) 7.46 (m, 10H, PPh_3–Phenyl) 3.68 (m, 2H, –SCH_2CH_2S), 2.78 (m, 4H, –SCH_2CH_2S) 1.83 (m, 2H, –SCH_2CH_2S). ^{13}C NMR (CD_2Cl_2) δ: 134.67, 130.93, 128.5, 45.7. ^{31}P (CD_2Cl_2) δ: 33.0. Elemental analysis: ($C_{22}H_{23}NPS_3Re$) theory (C: 42.98; N: 2.28, H: 3.77). Found (C: 43.69, N: 1.99, H: 3.81). Because of a slight impurity from technical grade 2,2 thiodiethanethiol, these results are outside the range viewed as establishing analytical purity, they are provided to illustrate the best values obtained to date.

Synthesis of 2a. In a 25 ml scintillation vial, **1**, (50 mg, 0.081 mmol) was dissolved in 10 mL of benzene. Trispentafluorophenylborane (1 equiv. 0.081 mmol, 42.0 mg) was added to the reaction mixture, which was allowed to stir at room temperature for 15 min. Solvent was removed under reduced pressure and the resulting red residue was washed with pentane and dried *in vacuo* to afford **2** as a red powder. X-ray quality crystals were obtained by vapor diffusion of pentane into a concentrated CH_2Cl_2 solution. Isolated (57 mg, 62% yield) (^{1}H NMR (CD_2Cl_2) δ: 7.53 (m, 8H, PPh_3–Phenyl), 7.32 (m, 7H, PPh_3–Phenyl), 4.07 (m, 2H, –SCH_2CH_2S) 3.66 (m, 2H, –SCH_2CH_2S) 2.98 (m, 2H, –SCH_2CH_2S) 1.99 (m, 2H, –SCH_2CH_2S). ^{13}C NMR (CD_2Cl_2) δ: 44.28, 46.12, 128.42, 131.59, 134.83. ^{19}F NMR (CD_2Cl_2) −131.0 (d, 2F) −160.4 (t, 1F) −165.8 (m, 2F) ^{31}P (CD_2Cl_2), δ: 30.9. Elemental analysis: ($C_{40}H_{23}BF_{15}NPS_3Re$) theory (C: 42.64; N: 1.24, H: 2.06), found (C: 42.26, N: 1.22, H: 1.76).

Generation of 2b. In a screw cap NMR tube equipped with a Teflon cap, **1** (15 mg, 0.024 mmol) and $Al(C_6F_5)_3$·toluene (14.9 mg, 0.024 mmol) were dissolved in C_6D_6. The reaction was accompanied by an instant color change from yellow to red. ^{1}H NMR (C_6D_6) δ: 7.62 (bs, 5H, PPh3), 6.92 (m, 10H, PPh_3) 3.22 (m, 2H, –SCH_2CH_2S) 2.63 (m, 2H, –SCH_2CH_2S) 2.27 (m, 2H, –SCH_2CH_2S) 0.61 (m, 2H, –SCH_2CH_2S). ^{31}P NMR (C_6D_6) δ: 29.9; ^{19}F NMR (C_6D_6) δ: −120.9 (m, 2F) −154.7 (m, 1F) −162.4 (m, 2F).

Generation of 2c. In a screw cap NMR tube equipped with a Teflon cap, **1** (15 mg, 0.024 mmol) and $Zn(C_6F_5)_2$ (9.6 mg, 0.024 mmol) were dissolved in C_6D_6. The reaction was accompanied by an instant color change from yellow to red. ^{1}H NMR (C_6D_6) δ: 7.70 (m, 5H, PPh_3), 7.01 (m, 10H, PPh_3) 3.18 (m, 2H, –SCH_2CH_2S) 2.43 (m, 2H, –SCH_2CH_2S) 2.32 (m, 2H, –SCH_2CH_2S) 0.74 (m, 2H, –SCH_2CH_2S). ^{31}P NMR (C_6D_6) δ: 28.9. ^{19}F NMR (C_6D_6) δ: −116.5 (m, 2F) −156.3 (m, 1F) −161.7 (m, 2F).

Synthesis of 3. In a 25 ml scintillation vial, (SSS)Re(N)PPh_3 (50 mg, 0.081 mmol) was dissolved in 10 mL of benzene. Triphenylcarbenium tetrafluoroborate (1 equiv. 0.081 mmol, 27 mg) was added to the reaction mixture, which was allowed to stir at room temperature for 15 min. Solvent was removed under reduced pressure and the following yellow residue was redissolved in 10 mL of CH_2Cl_2. Addition of excess Et_2O precipitated the product as a yellow powder that was collected on a filter frit and dried *in vacuo*. Isolated (47 mg, 61% yield). ^{1}H NMR (CD_2Cl_2) δ: 7.54–7.19 (m, 25H, PPh3–Phenyl and CPh_3–Phenyl) 6.80 (m, 5H, PPh3–Phenyl) 4.26 (m, 2H, –SCH_2CH_2S) 3.73 (m, 2H, –SCH_2CH_2S) 3.28 (m, 2H, –SCH_2CH_2S) 2.37 (m, 2H, –SCH_2CH_2S). ^{31}P (CD_2Cl_2) δ: 30.1. Elemental analysis: ($C_{41}H_{38}NPS_3ReBF_4$) theory (C: 52.12; N: 1.48, H: 4.05), found (C: 52.21, N: 1.58, H: 4.16).

Synthesis of 4. In a 25 ml scintillation vial, (SSS)Re(N)PPh_3 (90 mg, 0.15 mmol) was dissolved in 10 mL of benzene. Tertbutyl isonitrile (2 equiv. 0.29 mmol, 40 μL) was added to the reaction mixture, which was allowed to stir at reflux temperature overnight. Solvent was removed under reduced pressure and the following yellow residue was redissolved in 10 mL of methanol. Insoluble PPh_3 was removed by filtering the solution through Celite plug and the residual solution was allowed to evaporate at room temperature. Isolated (25 mg, 38% yield). ^{1}H NMR (CD_2Cl_2) δ: 7.74 (m, 5H, PPh_3–Phenyl), 7.46 (m, 10H, PPh_3–Phenyl) 3.68 (m, 4H, –SCH_2CH_2S) 2.78 (m, 2H, –SCH_2CH_2S) 1.83 (m, 4H, –SCH_2CH_2S). ^{13}C NMR (CD_2Cl_2) δ: 134.67, 130.93, 128.5, 45.7. Successful elemental analysis could not be obtained for this molecule.

Generation of 5a. In a screw cap NMR tube equipped with a Teflon cap, **4** (15 mg, 0.034 mmol) and $B(C_6F_5)_3$ (17.6 mg, 0.024 mmol) were dissolved in C_6D_6. The reaction was accompanied by an instant color change from yellow to red. ^{1}H NMR (C_6D_6) δ: 3.23 (m, 2H, –SCH_2CH_2S) 2.60 (m, 2H, –SCH_2CH_2S) 2.24 (m, 2H, –SCH_2CH_2S) 0.87 (s, 9H, *t*-BuNC) 0.78 (m, 2H, –SCH_2CH_2S). ^{19}F NMR (C_6D_6) δ: −131.1 (m, 2F) −158.8 (m, 1F) −164.4 (m, 2F).

Generation of 5b. In a screw cap NMR tube equipped with a Teflon cap, **4** (15 mg, 0.034 mmol) and $Al(C_6F_5)_3$·toluene (21.1 mg, 0.024 mmol) were dissolved in C_6D_6. The reaction was accompanied by an instant color change from yellow to red. ^{1}H NMR (C_6D_6) δ: 3.24 (m, 2H, –SCH_2CH_2S) 2.59 (m, 2H, –SCH_2CH_2S) 2.27 (m, 2H, –SCH_2CH_2S) 0.85 (s, 9H, *t*-BuNC) 0.78 (m, 2H, –SCH_2CH_2S). ^{19}F NMR (C_6D_6) δ: −121.8 (m, 2F) −154.0 (m, 1F) −162.1 (m, 2F).

Computational details

Geometry and transition state optimizations were performed with the 6-31G(d,p)[19] basis set on light atoms and the SDD[20] basis set with an added *f* polarization function on rhenium.[21] Each optimization involved tight optimization criteria implemented in Gaussian 09 [22] (opt = tight) with an ultrafine integral grid (int = ultrafine) and the M06 functional.[16] All structures were fully optimized and analytical frequency calculations were performed on all structures to ensure either a zeroth order saddle point (a local minimum) or a first order saddle point (a transition state). The minima associated with each transition state were determined by animation of the imaginary frequency. Energetics were calculated at 298 K with the 6-311++G(d,p)[23] basis set for C, H, N, O, P atoms and the SDD basis set with an added *f* polarization function on Re with the M06 functional. Reported energies utilized analytical frequencies and the zero point corrections from the gas phase optimized geometries and include solvation corrections which were computed using the PCM method,[24] with methylene chloride as the solvent as implemented in Gaussian 09.

Conflicts of interest

There are no conflicts to declare.

Acknowledgements

We acknowledge North Carolina State University and the National Science Foundation *via* (CHE-1664973) for funding. We also acknowledge the NCSU High Performance Computing Center (HPC) for computational support.

Notes and references

1 (*a*) T. D. Lohrey, R. G. Bergman and J. Arnold, *Inorg. Chem.*, 2016, **55**, 11993–12000; (*b*) D. D. Wright and S. N. Brown, *Inorg. Chem.*, 2013, **52**, 7831–7833; (*c*) L. D. McPherson, M. Drees, S. I. Khan, T. Strassner and M. M. Abu-Omar, *Inorg. Chem.*, 2004, **43**, 4036–4050; (*d*) Y. Wang and J. H. Espenson, *Inorg. Chem.*, 2002, **41**, 2266–2274; (*e*) W.-D. Wang, I. A. Guzei and J. H. Espenson, *Organometallics*, 2001, **20**, 148–156; (*f*) J. C. Bryan, R. E. Stenkamp, T. Tulip and J. M. Mayer, *Inorg. Chem.*, 1987, **26**, 2283–2288.

2 (*a*) G. Du and M. M. Abu-Omar, *Curr. Org. Chem.*, 2008, **12**, 1185–1198; (*b*) E. A. Ison, E. R. Trivedi, R. A. Corbin and M. M. Abu-Omar, *J. Am. Chem. Soc.*, 2005, **127**, 15374–15375.

3 (*a*) T. A. Fernandes, J. R. Bernardo and A. C. Fernandes, *ChemCatChem*, 2015, **7**, 1177–1183; (*b*) S. Bi, J. Wang, L. Liu, P. Li and Z. Lin, *Organometallics*, 2012, **31**, 6139–6147.

4 (*a*) S. Liu, J. Yi and M. M. Abu-Omar, *Reaction Pathways and Mechanisms in Thermocatalytic Biomass Conversion II*, Springer, 2016, pp. 1–11; (*b*) T. Nakagiri, M. Murai and K. Takai, *Org. Lett.*, 2015, **17**, 3346–3349; (*c*) L. Sandbrink, E. Klindtworth, H.-U. Islam, A. M. Beale and R. Palkovits, *ACS Catal.*, 2015, **6**, 677–680; (*d*) J. R. Dethlefsen and P. Fristrup, *ChemSusChem*, 2015, **8**, 767–775; (*e*) S. Raju, M.-E. Moret and R. J. M. Klein Gebbink, *ACS Catal.*, 2014, **5**, 281–300; (*f*) S. Liu, A. Senocak, J. L. Smeltz, L. Yang, B. Wegenhart, J. Yi, H. I. Kenttämaa, E. A. Ison and M. M. Abu-Omar, *Organometallics*, 2013, **32**, 3210–3219; (*g*) I. Ahmad, G. Chapman and K. M. Nicholas, *Organometallics*, 2011, **30**, 2810–2818; (*h*) E. Arceo, J. A. Ellman and R. G. Bergman, *J. Am. Chem. Soc.*, 2010, **132**, 11408–11409; (*i*) S. Vkuturi, G. Chapman, I. Ahmad and K. M. Nicholas, *Inorg. Chem.*, 2010, **49**, 4744–4746.

5 (*a*) B. D. Sherry, R. N. Loy and F. D. Toste, *J. Am. Chem. Soc.*, 2004, **126**, 4510–4511; (*b*) J. J. Kennedy-Smith, L. A. Young and F. D. Toste, *Org. Lett.*, 2004, **6**, 1325–1327; (*c*) B. D. Sherry, A. T. Radosevich and F. D. Toste, *J. Am. Chem. Soc.*, 2003, **125**, 6076–6077; (*d*) M. R. Luzung and F. D. Toste, *J. Am. Chem. Soc.*, 2003, **125**, 15760–15761.

6 H. Jin, J. Xie, C. Pan, Z. Zhu, Y. Cheng and C. Zhu, *ACS Catal.*, 2013, **3**, 2195–2198.

7 (*a*) N. S. Lambic, R. D. Sommer and E. A. Ison, *ACS Catal.*, 2017, **7**, 1170–1180; (*b*) N. S. Lambic, R. D. Sommer and E. A. Ison, *J. Am. Chem. Soc.*, 2016, **138**, 4832–4842.

8 R. A. Eikey and M. M. Abu-Omar, *Coord. Chem. Rev.*, 2003, **243**, 83–124.

9 (*a*) H. H. Nguyen, T. N. Trieu and U. Abram, *Z. Anorg. Allg. Chem.*, 2011, **637**, 1330–1333; (*b*) H. Braband and U. Abram, *Chem. Commun.*, 2003, 2436–2437; (*c*) K. Frick, U. Ziener and M. Hanack, *Eur. J. Inorg. Chem.*, 1999, **1999**, 1309–1313; (*d*) A. Neuhaus, A. Veldkamp and G. Frenking, *Inorg. Chem.*, 1994, **33**, 5278–5286; (*e*) P. J. Blower and J. R. Dilworth, *Dalton Trans.*, 1985, 2305–2309.

10 (*a*) U. Abram, B. Schmidt-Brücken, A. Hagenbach, M. Hecht, R. Kirmse and A. Voigt, *Z. Anorg. Allg. Chem.*, 2003, **629**, 838–852; (*b*) U. Abram, A. Voigt and R. Kirmse, *Polyhedron*, 2000, **19**, 1741–1748; (*c*) U. Abram, B. Schmidt-Brücken and S. Ritter, *Polyhedron*, 1999, **18**, 831–838.

11 J. L. Smeltz, C. P. Lilly, P. D. Boyle and E. A. Ison, *J. Am. Chem. Soc.*, 2013, **135**, 9433–9441.

12 (*a*) N. S. Lambic, C. P. Lilly, R. D. Sommer and E. A. Ison, *Organometallics*, 2016, **35**, 3060–3068; (*b*) N. S. Lambic, C. P. Lilly, L. K. Robbins, R. D. Sommer and E. A. Ison, *Organometallics*, 2016, **35**, 2822–2829; (*c*) L. K. Robbins, C. P. Lilly, R. D. Sommer and E. A. Ison, *Organometallics*, 2016, **35**, 3530–3537; (*d*) L. K. Robbins, C. P. Lilly, J. L. Smeltz, P. D. Boyle and E. A. Ison, *Organometallics*, 2015, **34**, 3152–3158; (*e*) J. L. Smeltz, C. E. Webster and E. A. Ison, *Organometallics*, 2012, **31**, 4055–4062; (*f*) C. P. Lilly, P. D. Boyle and E. A. Ison, *Organometallics*, 2012, **31**, 4295–4301; (*g*) J. L. Smeltz, P. D. Boyle and E. A. Ison, *J. Am. Chem. Soc.*, 2011, **133**, 13288–13291.

13 A. Boschi, E. Cazzola, L. Uccelli, M. Pasquali, V. Ferretti, V. Bertolasi and A. Duatti, *Inorg. Chem.*, 2012, **51**, 3130–3137.

14 L. H. Doerrer, A. J. Graham and M. L. H. Green, *Dalton Trans.*, 1998, 3941–3946.

15 W.-H. Leung, J. L. C. Chim, I. D. Williams and W.-T. Wong, *Inorg. Chem.*, 1999, **38**, 3000–3005.

16 Y. Zhao and D. G. Truhlar, *Theor. Chem. Acc.*, 2008, **120**, 215–241.

17 J. C. Bryan, R. E. Stenkamp, T. Tulip and J. M. Mayer, *Inorg. Chem.*, 1987, **26**, 2283–2288.

18 J. M. Mayer, *Inorg. Synth.*, 1993, **29**, 146–150.

19 V. A. Rassolov, M. A. Ratner, J. A. Pople, P. C. Redfern and L. A. Curtiss, *J. Comput. Chem.*, 2001, **22**, 976–984.

20 D. Andrae, U. Haeussermann, M. Dolg, H. Stoll and H. Preuss, *Theor. Chem. Acc.*, 1990, **77**, 123–141.

21 A. Ehlers, M. Böhme, S. Dapprich, A. Gobbi, A. Höllwarth, V. Jonas, K. Köhler, R. Stegmann, A. Veldkamp and G. Frenking, *Chem. Phys. Lett.*, 1993, **208**, 111–114.

22 M. J. Frisch, G. W. Trucks, H. B. Schlegel, G. E. Scuseria, M. A. Robb, J. R. Cheeseman, G. Scalmani, V. Barone, B. Mennucci, G. A. Petersson, H. Nakatsuji, M. Caricato, X. Li, H. P. Hratchian, A. F. Izmaylov, J. Bloino, G. Zheng,

J. L. Sonnenberg, M. Hada, M. Ehara, K. Toyota, R. Fukuda, J. Hasegawa, M. Ishida, T. Nakajima, Y. Honda, O. Kitao, H. Nakai, T. Vreven, J. A. Montgomery Jr., J. E. Peralta, F. Ogliaro, M. Bearpark, J. J. Heyd, E. Brothers, K. N. Kudin, V. N. Staroverov, R. Kobayashi, J. Normand, K. Raghavachari, A. Rendell, J. C. Burant, S. S. Iyengar, J. Tomasi, M. Cossi, N. Rega, M. J. Millam, M. Klene, J. E. Knox, J. B. Cross, V. Bakken, C. Adamo, J. Jaramillo, R. Gomperts, R. E. Stratmann, O. Yazyev, A. J. Austin, R. Cammi, C. Pomelli, J. W. Ochterski, R. L. Martin, K. Morokuma, V. G. Zakrzewski, G. A. Voth, P. Salvador, J. J. Dannenberg, S. Dapprich, A. D. Daniels, Ö. Farkas, J. B. Foresman, J. V. Ortiz, J. Cioslowski and D. J. Fox, *Gaussian 09, Revision D.01*, Gaussian, Inc., Wallingford CT, 2009.

23 M. M. Francl, W. J. Pietro, W. J. Hehre, J. S. Binkley, M. S. Gordon, D. J. DeFrees and J. A. Pople, *J. Chem. Phys.*, 1982, **77**, 3654–3665.

24 J. Tomasi, B. Mennucci and E. Cances, *J. Mol. Struct.: THEOCHEM*, 1999, **464**, 211–226.